Thermal Diffusion and Chemical Reaction Effects on Free Convection MHD Flow through a Porous Medium bounded by a Vertical Surface with Constant Heat Flux

P. K. Sahu and U. S. Rajput

Abstract—**The combined effects of thermal diffusion and chemical reaction on the steady free convection MHD flow through a porous medium bounded by an infinite vertical surface with constant heat flux are studied here. The governing equations involved in the present analysis are solved by the two-term perturbation method for the velocity, temperature and concentration field. The numerical values of the skin friction and Sherwood number have been tabulated. The effects of various parameters associated with flow like thermal Grashof number, mass Grashof number, Schmidt number, magnetic field parameter, permeability parameter, Prandtl number, Eckert number, chemical reaction parameter and Soret number are studied with the help of graphs and tables.**

***Keywords*—Chemical reaction, Free convection, MHD, Porous medium and Thermal diffusion.**

***MSC 2010 Codes* — 74F25, 76R10, 76W05 and 76S05.**

I. INTRODUCTION

The MHD heat and mass transfer, which occur due to buoyancy forces caused by temperature difference and concentration difference, play a decisive role in power engineering, metallurgy, drying of solid materials, extraction, condensation, rectification, evaporation, distillation and absorption of a fluid. Sattar and Alam [1] have presented an unsteady MHD free convective heat and mass transfer flow with hall current of an electrically conducting incompressible viscous fluid through a porous medium along an infinite vertical porous plate with constant heat flux.

Muthucumaraswamy et al. [2] have presented heat and mass transfer effects on flow past an impulsively started infinite vertical plate in the presence of uniform heat and mass flux at the plate. Chemical reaction effects on moving infinite vertical plate with uniform heat flux and variable mass diffusion were studied by Muthucumaraswamy and Kulandaivel [3]. Muthucumaraswamy et al. [4] have studied mass transfer effects on exponentially accelerated isothermal vertical plate.

Free convection flows are frequently encountered in physical and engineering problems such as chemical catalytic reactors, nuclear waste materials, geothermal systems etc. Chaudhary et al. [5] have presented the free convection flow of a viscous incompressible fluid past an infinite vertical accelerated plate embedded in porous medium with constant heat flux in the presence of transverse magnetic field. Singh and Kumar [6] have presented the effects of chemical reactions on unsteady MHD free convection and mass transfer flow of a viscous, incompressible, electrically-conducting fluid past an infinite hot vertical porous plate embedded in porous medium with heat generation/absorption. Rajvanshi and Saini [7] have studied free convection MHD flow past a uniformly moving infinite vertical porous surface with gravity modulation at constant heat flux. Mahapatra et al. [8] have studied the effect of chemical reaction on free convection flow through a porous medium bounded by vertical surface.

This problem was further extended for magnetohydrodynamic case by Rajput and Surendra [9]. Sengupta [10] studied the combined effect of thermal diffusion and heat absorption on the free convection mass transfer flow of a viscous incompressible fluid past a continuously moving infinite porous plate. Haque et al. [11] have presented MHD free convective heat generating unsteady micropolar fluid flow through a porous medium with constant heat and mass fluxes. Further, we [12] have presented the effects of chemical reactions on free convection MHD flow of a viscous incompressible electrically conducting fluid past an exponentially accelerated infinite vertical plate through a porous medium with variable temperature and mass diffusion.

The main objective of the present work is to investigate thermal diffusion and chemical reaction effects on the steady free convection MHD flow of an incompressible viscous electrically conducting fluid through a porous medium bounded by an infinite vertical surface with constant heat flux.

P. K. Sahu is with the Department of Mathematics and Astronomy, University of Lucknow, Lucknow - 226007, U. P., India. (phone: +91-8604667822; e-mail: ppradeepsahu2010@gmail.com).

U. S. Rajput is with the Department of Mathematics and Astronomy, University of Lucknow, Lucknow - 226007, U. P., India. (phone: +91-8604822512; e-mail: rajputpradeeplko@gmail.com).

II. MATHEMATICAL ANALYSIS

We consider a steady flow of an incompressible viscous electrically conducting fluid through a porous medium occupying a semi-infinite region of the space bounded by a vertical infinite surface with constant heat flux in the presence of a transversely imposed magnetic field B_0 and thermal diffusion. Introduce a co-ordinate system (x', y') with x'-axis along the length of the plate (vertical surface) in the upward vertical direction and y'- axis normal to the plate (vertical surface) towards the fluid region. The plate is subjected to a constant suction parallel to y'- axis. The fluid properties are assumed to be constant except for the density in the body force term. Further, a chemically reactive species is emitted from the vertical surface into a hydrodynamic flow field. It diffuses into the fluid, where it undergoes a homogeneous chemical reaction. The reaction is assumed to take place entirely in the stream. Then under the above assumption and Boussinesq's approximation, the flow is governed by following equations:

$$\frac{\partial v'}{\partial y'} = 0, \tag{1}$$

$$v'\frac{\partial u'}{\partial y'} = \nu\frac{\partial^2 u'}{\partial y'^2} + g\beta(T' - T'_\infty) + g\beta^*(C' - C'_\infty) - \frac{\sigma B_0^2}{\rho}u' - \frac{\nu u'}{K_p}, \tag{2}$$

$$v'\frac{\partial T'}{\partial y'} = \frac{\alpha}{\rho C_p}\frac{\partial^2 T'}{\partial y'^2} + \frac{\nu}{C_p}\left(\frac{\partial u'}{\partial y'}\right)^2, \tag{3}$$

$$v'\frac{\partial C'}{\partial y'} = D\frac{\partial^2 C'}{\partial y'^2} + D_T\frac{\partial^2 T'}{\partial y'^2} - K_l(C' - C'_\infty). \tag{4}$$

Equation (1) gives

$$v' = \text{Constant}\ (= -v_0,\ \text{say}), \tag{5}$$

where $v_0 > 0$ and v' is the steady normal velocity of suction on the surface.

The corresponding boundary conditions are:

$$\left.\begin{aligned} &u' = 0,\ \frac{\partial T'}{\partial y'} = -\frac{q}{\alpha},\ C' = C'_w \quad \text{at}\ \ y' = 0,\\ &u' \to 0,\ T' \to T'_\infty,\ C' \to C'_\infty \quad \text{as}\ \ y' \to \infty. \end{aligned}\right\} \tag{6}$$

Let us introduce the following non-dimensional parameters:

$$\left.\begin{aligned} &u = \frac{u'}{v_0},\ y = \frac{v_0 y'}{\nu},\ \theta = \frac{\alpha v_0(T' - T'_\infty)}{q\nu},\ C = \frac{C' - C'_\infty}{C'_w - C'_\infty},\\ &Gr = \frac{g\beta q\nu^2}{v_0^4\alpha},\ Gc = \frac{g\beta^*\nu(C'_w - C'_\infty)}{v_0^3}, \Pr = \frac{\rho\nu C_p}{\alpha},\\ &Sc = \frac{\nu}{D},\ M = \frac{\sigma B_0^2\nu}{\rho v_0^2},\ K = \frac{K_p v_0^2}{\nu^2},\ E = \frac{\alpha v_0^3}{C_p\nu q},\\ &Kc = \frac{\nu K_l}{v_0^2},\ Sr = \frac{D_T q}{\alpha v_0(C'_w - C'_\infty)}. \end{aligned}\right\} \tag{7}$$

Using above dimensionless quantities, the governing equations (1)–(4) are reduced to the following non-dimensional form:

$$\frac{\partial^2 u}{\partial y^2} + \frac{\partial u}{\partial y} - \left(M + \frac{1}{K}\right)u = -Gr\theta - GcC, \tag{8}$$

$$\frac{\partial^2\theta}{\partial y^2} + \Pr\frac{\partial\theta}{\partial y} = -\Pr.E\left(\frac{\partial u}{\partial y}\right)^2, \tag{9}$$

$$\frac{\partial^2 C}{\partial y^2} + Sc\frac{\partial C}{\partial y} - ScKcC = -ScSr\frac{\partial^2\theta}{\partial y^2}. \tag{10}$$

The corresponding boundary conditions in the dimensionless form can be written as:

$$\left.\begin{aligned} &u = 0,\ \frac{\partial\theta}{\partial y} = -1,\ C = 1 \quad \text{at}\ \ y = 0,\\ &u \to 0,\ \theta \to 0,\ C \to 0 \quad \text{as}\ \ y \to \infty. \end{aligned}\right\} \tag{11}$$

The dimensionless governing equations (8), (9) and (10) subject to the boundary conditions (11), are coupled, non-linear partial differential equations and these cannot be solved in closed-form. However, these equations can be reduced to a set of ordinary differential equations with the help of perturbation method, which can be solved analytically. Expand u, θ, and C in power of the Eckert number E (assuming that E is very small), we can write:

$$\left.\begin{aligned} u &= u_0 + Eu_1 + o(E^2),\\ \theta &= \theta_0 + E\theta_1 + o(E^2),\\ C &= C_0 + EC_1 + o(E^2). \end{aligned}\right\} \tag{12}$$

Substituting the equation (12) into equations (8)–(10), equating the coefficients at the terms with the same powers of E, and neglecting terms of the order of E^2 and above, we get the following equations:

Zero order:

$$\frac{\partial^2 u_0}{\partial y^2}+\frac{\partial u_0}{\partial y}-mu_0=-Gr\theta_0-GcC_0, \tag{13}$$

$$\frac{\partial^2 \theta_0}{\partial y^2}+\Pr\frac{\partial \theta_0}{\partial y}=0, \tag{14}$$

$$\frac{\partial^2 C_0}{\partial y^2}+Sc\frac{\partial C_0}{\partial y}-ScKcC_0=-ScSr\frac{\partial^2 \theta_0}{\partial y^2}. \tag{15}$$

First order:

$$\frac{\partial^2 u_1}{\partial y^2}+\frac{\partial u_1}{\partial y}-mu_1=-Gr\theta_1-GcC_1, \tag{16}$$

$$\frac{\partial^2 \theta_1}{\partial y^2}+\Pr\frac{\partial \theta_1}{\partial y}=-\Pr\left(\frac{\partial u_0}{\partial y}\right)^2, \tag{17}$$

$$\frac{\partial^2 C_1}{\partial y^2}+Sc\frac{\partial C_1}{\partial y}-ScKcC_1=-ScSr\frac{\partial^2 \theta_1}{\partial y^2}, \tag{18}$$

where $m=M+\dfrac{1}{K}$.

The corresponding boundary conditions are as follows:

$$\left.\begin{aligned} &u_0=0,\quad u_1=0,\quad \frac{\partial\theta_0}{\partial y}=-1,\quad \frac{\partial\theta_1}{\partial y}=0,\\ &C_0=1,\ C_1=0 \quad \text{at} \quad y=0,\\ &u_0\to 0,\ u_1\to 0,\quad \theta_0\to 0,\quad \theta_1\to 0,\\ &C_0\to 0,\ C_1\to 0 \ \text{ as } \ y\to\infty. \end{aligned}\right\} \tag{19}$$

Solving equations (13) - (18) under the boundary conditions (19), and then using (12), we get the solution, which is as under:

$$\begin{aligned} u(y)=&A_2\exp(-\alpha y)-G_1\exp(-\Pr y)\\ &-G_2(1+A_1)\exp(-\lambda y)+G_3A_1\exp(-\Pr y)\\ &+E\left[A_{32}\exp(-\alpha y)+A_{24}\exp(-\Pr y)\right.\\ &+A_{25}\exp(-2\alpha y)+A_{26}\exp(-2\lambda y)+A_{27}\exp(-2\Pr y)\\ &+A_{28}\exp(-(\alpha+\lambda)y)+A_{29}\exp(-(\lambda+\Pr)y)\\ &\left.+A_{30}\exp(-(\Pr+\alpha)y)-A_{31}\exp(-\lambda y)\right], \end{aligned} \tag{20}$$

$$\begin{aligned} \theta(y)=&\frac{\exp(-\Pr y)}{\Pr}+E\left[A_{15}\exp(-\Pr y)\right.\\ &-A_9\exp(-2\alpha y)-A_{10}\exp(-2\lambda y)\\ &-A_{11}\exp(-2\Pr y)+A_{12}\exp(-(\alpha+\lambda)y)\\ &\left.-A_{13}\exp(-(\lambda+\Pr)y)+A_{14}\exp(-(\Pr+\alpha)y)\right], \end{aligned} \tag{21}$$

$$\begin{aligned} C(y)=&(1+A_1)\exp(-\lambda y)-A_1\exp(-\Pr y)\\ &+E\left[A_{23}\exp(-\lambda y)-A_{16}\exp(-\Pr y)\right.\\ &+A_{17}\exp(-2\alpha y)+A_{18}\exp(-2\lambda y)\\ &+A_{19}\exp(-2\Pr y)-A_{20}\exp(-(\alpha+\lambda)y)\\ &\left.+A_{21}\exp(-(\lambda+\Pr)y)-A_{22}\exp(-(\Pr+\alpha)y)\right]. \end{aligned} \tag{22}$$

The non-dimensional skin-friction or the wall shear stress at the surface is given by:

$$\begin{aligned} \tau=\left(\frac{\partial u}{\partial y}\right)_{y=0}=&-\alpha A_2+\Pr G_1+\lambda(1+A_1)G_2\\ &-\Pr A_1G_3+E\left[-\Pr A_{24}-2\alpha A_{25}-2\lambda A_{26}\right.\\ &-2\Pr A_{27}-(\alpha+\lambda)A_{28}-(\lambda+\Pr)A_{29}\\ &\left.-(\Pr+\alpha)A_{30}+\lambda A_{31}-\alpha A_{32}\right]. \end{aligned} \tag{23}$$

The non-dimensional Sherwood number is given by:

$$\begin{aligned} Sh=-\left(\frac{\partial C}{\partial y}\right)_{y=0}=&(1+A_1)\lambda-A_1\Pr\\ &+E\left[A_{23}\lambda-A_{16}\Pr+2A_{17}\alpha+2A_{18}\lambda+2A_{19}\Pr\right.\\ &\left.-(\alpha+\lambda)A_{20}+(\lambda+\Pr)A_{21}-(\Pr+\alpha)A_{22}\right]. \end{aligned} \tag{24}$$

III. Results and Discussion

In order to get the physical insight in to the problem, the numerical values of the velocity, temperature, concentration, skin-friction and Sherwood number are computed for different parameters like thermal Grashof number Gr, mass Grashof number Gc, Schmidt number Sc, magnetic field parameter M, permeability parameter K, Prandtl number $\Pr$, Eckert number E, chemical reaction parameter Kc and Soret number Sr. The values of main parameters considered are: Thermal Grashof number Gr = 5.0, 10.0, 15.0; mass Grashof number Gc = 5.0, 10.0, 15.0; Schmidt number Sc = 0.22 (for hydrogen), 0.66 (for oxygen), 0.78 (for ammonia) and 2.01 (for ethyl Benzene); magnetic field parameter M = 1.0, 2.0, 3.0; permeability parameter K = 0.1, 0.4, 0.7, 1.0; Prandtl number $\Pr$ = 0.71 (for air), 3.0 (for the saturated liquid Freon at 273.3 K), 7.0 (for water); Eckert number E = -0.05, -0.01, 0.01, 0.05; chemical reaction parameter Kc = -0.04, -0.02, 0.05, 1.0; Soret number Sr = 0.0, 0.5, 1.0, 2.0.

The effects of the important flow parameters such as magnetic field parameter M, Soret number Sr, Eckert number E, mass Grashof number Gc, thermal Grashof number Gr, Schmidt number Sc, Prandtl number $\Pr$, chemical reaction parameter Kc and permeability parameter K on the velocity profiles of the flow field have been discussed with the help of figures 1 to 9, respectively. From figure 1, it is observed that the velocity of fluid increases as the value of magnetic field parameter M decreases (keeping other parameters Sr, E, Gc, Gr, Sc, $\Pr$, Kc and K constant). It is because that the application of transverse magnetic field will result a resistive type force (Lorentz force) similar to drag force, which tends to resist the fluid flow and thus reducing its velocity. This force has the tendency to slowdown the motion of the fluid in the boundary layer. The effect of Soret number Sr on the velocity of fluid u against y is shown in figure 2. It is seen that the velocity increases sharply due to increase in values of Sr and decreases steadily far away from the plate. The effects of the viscous dissipation parameter, i.e. the Eckert number E on the velocity field is shown in Figure 3. It is observed that the fluid velocity increases and reaches its maximum over a very short distance from the plate and then decreases gradually to zero as increasing y. Figures 4 and 5 represent the effects of mass Grashof number Gc and thermal Grashof number Gr on the velocity field, respectively. From these figures, it is observed that the velocity component near the plate increases with increase in mass Grashof number and thermal Grashof number, and after attaining a maximum value, it starts decreasing gradually. Figures 6 and 7 display the effect of Schmidt number Sc and Prandtl number $\Pr$ on the velocity profiles, respectively. The velocity for air $(\Pr = 0.71)$ is always greater than the water $(\Pr = 7.0)$ and liquid Freon ($\Pr = 3.0$). Physically, this is true because increase in the Prandtl number is due to the increase in the viscosity of the fluid which makes the fluid thick and hence causes a decrease in the velocity of the fluid. It is also observed that the fluid velocity decreases as the value of Schmidt number increases (keeping other parameters M, E, Gc, Gr, Sr, $\Pr$, Kc and K constant). Figure 8 shows the effect of the chemical reaction on the velocity profiles. A generative chemical reaction $(Kc < 0)$ increases the fluid flow velocity, whereas a destructive chemical reaction $(Kc > 0)$ reduces it. Figure 9 represents the effects of permeability parameter K on the velocity profiles. It is observed that the fluid velocity increases sharply and a peak value near to the plate and decays continuously as increasing y. It is also observed that the fluid velocity increases with increasing the permeability parameter.

The temperature profiles are illustrated in figures 10 to 15 for different values of Soret number Sr, magnetic field parameter M, Eckert number E, Prandtl number $\Pr$, permeability parameter K and thermal Grashof number Gr, respectively. Figure 10 and 12 represent that the temperature of fluid increases as the value of Soret number Sr and Eckert number E increase, respectively. From figure 11, it is clear that the temperature increases with the decrease of magnetic field parameter. In figure 13, it can be seen that the temperature of the fluid is inversely proportional to the value of Prandtl number $\Pr$. Thus, the increase in $\Pr$ reduces the temperature in the system. This is due to the fact that there would be a decrease of thermal boundary layer thickness with the increase of Prandtl number $\Pr$. Figures 14 and 15 represent that the temperature of the fluid increases as the value of permeability parameter K and thermal Grashof number Gr increase, respectively.

The effect of the Soret number Sr on the species concentration C is shown graphically in figure 16. Due to Soret effect the thickness of the concentration boundary layer raises, thereby increasing the value of C. The effect of Schmidt number Sc on concentration profiles is shown by figure 17. It is observed that concentration decreases with increase in Schmidt number *Sc*. The concentration field falls slowly and steadily. Figure 18 shows the effects of mass Grashof number Gc on concentration profile. It is observed that the concentration increases as the value of mass Grashof number increases. From figure 19, it is clear that a generative chemical reaction $(Kc < 0)$ increases the concentration of fluid, whereas a destructive chemical reaction $(Kc > 0)$ reduces it.

The effects of various parameters on the skin-friction are shown in tables 1 to 9. It is found from tables 1, 2 and 3 that the skin-friction increases with the rise of Soret number Sr, Eckert number E and permeability parameter K (keeping other parameters fixed), respectively. Further from tables 4, 5, 6 and 7, it is observed that the skin-friction decreases with the rise of Schmidt number Sc, Prandtl number $\Pr$, magnetic field parameter M and chemical reaction parameter Kc (keeping other parameters fixed), respectively. From tables 8 and 9, it is also observed that the skin-friction increases with the increase of mass Grashof number Gc and thermal Grashof number Gr. Again, the effect of various parameters like Soret number Sr, Schmidt number Sc and chemical reaction parameter Kc on the Sherwood number is shown in the tables 1, 4 and 7, respectively. From these tables, it is observed that the Sherwood number increases with the rise of Sc and Kc (keeping other parameters fixed) while, it decreases with increasing Sr (keeping other parameters fixed).

IV. Conclusion

In the present paper, a theoretical analysis has been done to study the combined effects of thermal diffusion and chemical reaction on the steady free convection MHD flow through a porous medium bounded by an infinite vertical surface with constant heat flux. Solutions for the model have been derived by using two- term perturbation method. The conclusion of the study is as follows:

- The velocity increases with increase in Sr, E, Gc, Gr and K, while it decreases with increase in M, Sc and $\Pr$.
- The temperature increases with increase in Sr, E, Gr and K, while it decreases with increase in M and $\Pr$.
- The concentration increases with increase in Sr and Gc, while it decreases with increase in Sc.
- The skin-friction increases with increase in Sr, E, K, Gc and Gr, while it decreases with increase in Sc, $\Pr$ and M.
- Sherwood number increases with increase in Sc, while it decreases with increase in Sr.
- Velocity, concentration and skin-friction coefficient increase and Sherwood number decreases for generative chemical reaction $(Kc < 0)$. However, destructive chemical reaction $(Kc > 0)$ have opposite effect on velocity, concentration, skin-friction and Sherwood number.

APPENDIX

$$m = M + \frac{1}{K},\ \alpha = \frac{1+\sqrt{1+4m}}{2},\ \lambda = \frac{Sc+\sqrt{Sc^2+4ScKc}}{2},$$

$$G_1 = \frac{Gr}{\Pr\left(\Pr^2-\Pr-m\right)}, G_2 = \frac{Gc}{\left(\lambda^2-\lambda-m\right)},$$

$$G_3 = \frac{Gc}{\left(\Pr^2-\Pr-m\right)},\ A_1 = \frac{ScSr\Pr}{\left(\Pr^2-Sc\Pr-ScKc\right)},$$

$$A_2 = G_1 + G_2(1+A_1) - G_3A_1,\ A_3 = A_2^2\alpha^2,$$

$$\mathrm{A}_4 = G_2^2\lambda^2(1+A_1)^2,\ \mathrm{A}_5 = \Pr^2(G_1-G_3A_1)^2,$$

$$\mathrm{A}_6 = 2A_2\alpha G_2\lambda(1+A_1),\ A_7 = 2G_2\lambda\Pr(1+A_1)(G_1-G_3A_1),$$

$$A_8 = 2A_2\alpha\Pr(G_1-G_3A_1), \mathrm{A}_9 = \frac{\Pr A_3}{\left(4\alpha^2-2\alpha\Pr\right)},$$

$$A_{10} = \frac{\Pr A_4}{\left(4\lambda^2-2\lambda\Pr\right)},\ \mathrm{A}_{11} = \frac{A_5}{2\Pr},\ \mathrm{A}_{12} = \frac{\Pr A_6}{\left\{(\alpha+\lambda)^2-(\alpha+\lambda)\Pr\right\}},$$

$$\mathrm{A}_{13} = \frac{\Pr A_7}{\left\{(\lambda+\Pr)^2-(\lambda+\Pr)\Pr\right\}},\ \mathrm{A}_{14} = \frac{\Pr A_8}{\left\{(\Pr+\alpha)^2-(\Pr+\alpha)\Pr\right\}},$$

$$A_{15} = \frac{1}{\Pr}\left[2\alpha A_9 + 2\lambda A_{10} + 2\Pr A_{11} - (\alpha+\lambda)A_{12} + (\lambda+\Pr)A_{13} - (\Pr+\alpha)A_{14}\right],$$

$$A_{16} = \frac{ScSrA_{15}\Pr^2}{\left(\Pr^2-Sc\Pr-ScKc\right)},\ A_{17} = \frac{4ScSrA_9\alpha^2}{\left(4\alpha^2-2\alpha Sc-ScKc\right)},$$

$$A_{18} = \frac{4ScSrA_{10}\lambda^2}{\left(4\lambda^2-2\lambda Sc-ScKc\right)}, A_{19} = \frac{4ScSrA_{11}\Pr^2}{\left(4\Pr^2-2\Pr Sc-ScKc\right)},$$

$$A_{20} = \frac{ScSrA_{12}(\alpha+\lambda)^2}{\left\{(\alpha+\lambda)^2-(\alpha+\lambda)Sc-ScKc\right\}},$$

$$A_{21} = \frac{ScSrA_{13}(\lambda+\mathrm{Pr})^2}{\left\{(\lambda+\mathrm{Pr})^2-(\lambda+\mathrm{Pr})Sc-ScKc\right\}},\ A_{22} = \frac{ScSrA_{14}(\mathrm{Pr}+\alpha)^2}{\left\{(\mathrm{Pr}+\alpha)^2-(\mathrm{Pr}+\alpha)Sc-ScKc\right\}},$$

$$A_{23} = A_{16} - A_{17} - A_{18} - A_{19} + A_{20} - A_{21} + A_{22},$$

$$\mathrm{A}_{24} = \frac{GcA_{16} - GrA_{15}}{\left(\mathrm{Pr}^2-\mathrm{Pr}-m\right)},\ \mathrm{A}_{25} = \frac{GrA_9 - GcA_{17}}{\left(4\alpha^2-2\alpha-m\right)},$$

$$\mathrm{A}_{26} = \frac{GrA_{10} - GcA_{18}}{\left(4\lambda^2-2\lambda-m\right)},\ \mathrm{A}_{27} = \frac{GrA_{11} - GcA_{19}}{\left(4\,\mathrm{Pr}^2-2\,\mathrm{Pr}-m\right)},$$

$$\mathrm{A}_{28} = \frac{GcA_{20} - GrA_{12}}{\left\{(\alpha+\lambda)^2-(\alpha+\lambda)-m\right\}},\ \mathrm{A}_{29} = \frac{GrA_{13} - GcA_{21}}{\left\{(\lambda+\mathrm{Pr})^2-(\lambda+\mathrm{Pr})-m\right\}},$$

$$\mathrm{A}_{30} = \frac{GcA_{22} - GrA_{14}}{\left\{(\mathrm{Pr}+\alpha)^2-(\mathrm{Pr}+\alpha)-m\right\}},\ \mathrm{A}_{31} = \frac{GcA_{23}}{\left(\lambda^2-\lambda-m\right)},$$

$$A_{32} = -A_{24} - A_{25} - A_{26} - A_{27} - A_{28} - A_{29} - A_{30} + A_{31}.$$

NOMENCLATURE

x', y'	Space co-ordinate
y	Dimensionless space co-ordinate
u', v'	Velocity components
u	Non-dimensional velocity
v_0	Suction velocity
C	Non-dimensional fluid concentration
C'	Concentration
C'_∞	Fluid concentration far away from the wall
T'	Temperature
T'_∞	Fluid temperature far away from the wall
D	Mass diffusivity
C_p	Specific heat at a constant pressure
E	Eckert number
K_p	Permeability of a porous medium
K	Non-dimensional permeability co-efficient of a porous medium
K_l	Rate of chemical reaction
Kc	Non-dimensional rate of a chemical reaction
Gc	Mass Grashof number
Gr	Thermal Grashof number
q	Rate of heat transfer
M	Magnetic field parameter
D_T	Thermal diffusivity
Sr	Soret number
Pr	Prandtl number
Sc	Schmidt number
Sh	Non-dimensional Sherwood number

Greek symbols

α	Thermal conductivity
β	Volumetric coefficient of thermal expansion
β^*	Volumetric coefficient of concentration expansion
ρ	Fluid density
θ	Non-dimensional temperature
τ	Non-dimensional skin-friction

Subscript

w	Conditions at wall
∞	Conditions far away from the wall.

REFERENCES

[1] M. A. Sattar, and M. M. Alam, "MHD free convection heat and mass transfer flow with Hall current and constant heat flux through a porous medium, " *Indian J. Pure Appl. Math*., 26(2), 1995, pp. 157-167.

[2] R. Muthucumaraswamy, P. Ganasan, and V. M. Soundalgekar, "Heat and mass transfer effects on flow past an impulsively started vertical plate," *Acta Mechanica*, 146, 2001, pp. 1-8.

[3] R. Muthucumaraswamy, and T. Kulandaivel, "Chemical reaction effects on moving infinite vertical plate with uniform heat flux and variable mass diffusion," *Forschung ingenieur,* vol. 68, 2003, pp. 101-104.

[4] R. Muthukumaraswamy, K. E. Sathappan, and R. Natarajan, "Mass transfer effects on exponentially accelerated isothermal vertical plate," *Int. J. Appl. Math. and Mech*., No. 64, 2008, pp. 19-25.

[5] R. C. Chaudhary, M. C. Goyal, and A. Jain, "Free convection effects on MHD flow past an infinite vertical accelerated plate embedded in porous media with constant heat flux, " *Mathematicas*, vol. XVII, No. 2, 2009, pp. 73-82.

[6] K. D. Sing, and R. Kumar, "Effects of chemical reactions on unsteady MHD free convection and mass transfer for flow past a hot vertical porous plate with heat generation/absorption through porous medium," Indian J. Phys., 83(1), 2010, pp. 93-106.

[7] S. C. Rajvanshi, and B. S. Saini, "Free convection MHD flow past a moving vertical porous surface with gravity modulation at constant heat flux," *Int. Journal of Theoretical & Applied Sciences*, 2(1), 2010, pp. 29-33.

[8] N. Mahapatra, G. C. Dash, S. Panda, and M. Acharya, "Effects of chemical reaction on free convection flow through a porous medium bounded by vertical surface." *Journal of Engineering Physics and Thermophysics*, vol. 83, No. 1, 2010, pp. 130-140.

[9] U. S. Rajput, and S. Kumar, "Effect of chemical reaction on free convection MHD flow through a porous medium bounded by vertical surface," *Elixir Appl. Math*., vol. 41, 2011, pp. 5957-5962.

[10] S. Sengupta, "Thermal diffusion effects on free convection mass transfer flow past a uniformly accelerated porous plate with heat sink," *Int. Journal of Mathematical Archive,* 2(8), 2011, pp. 1266-1276.
[11] M. M. Haque, M. M. Alam, M. Ferdows, and A. Postelnicu, "MHD free convection heat generating unsteady micropolar fluid flow through a porous medium with constant heat and mass fluxes," *European Journal of scientific Research ISSN 1450-216X*, vol. 53(3), 2011, pp. 491-515.
[12] U. S. Rajput, and P. K. Sahu, "Effects of chemical reactions on free convection MHD past an exponentially accelerated infinite vertical plate through a porous medium with variable temperature and mass diffusion," Elixir Appl. Math., vol. 43, 2012, pp. 6520-6527.

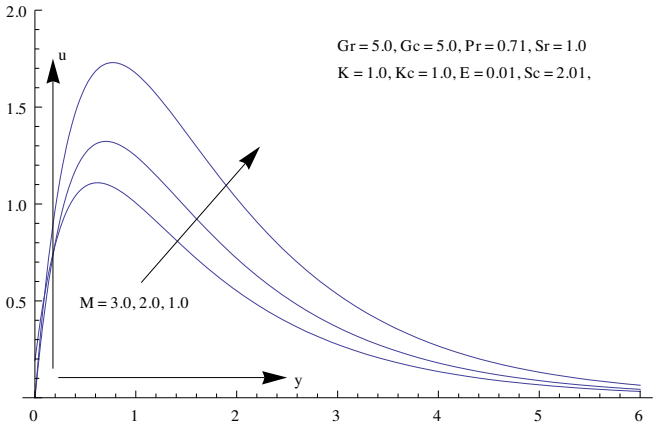

Figure-1: Velocity profiles for different M

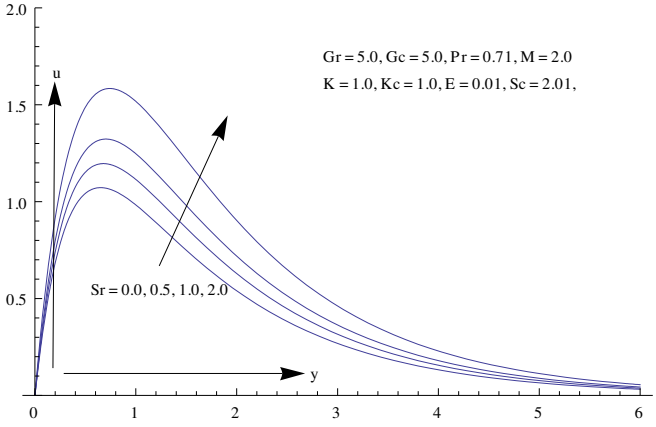

Figure-2: Velocity profiles for different Sr

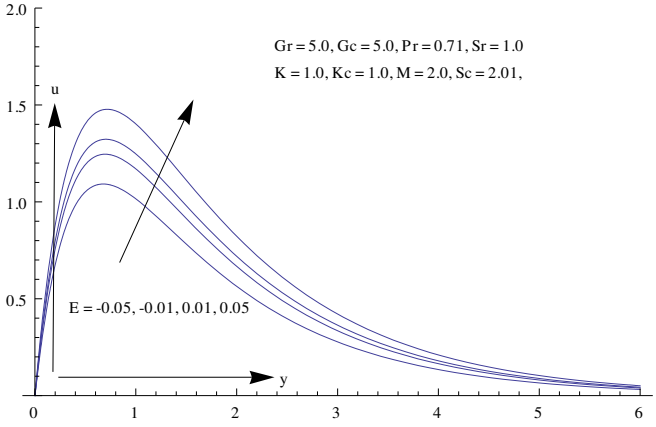

Figure-3: Velocity profiles for different E

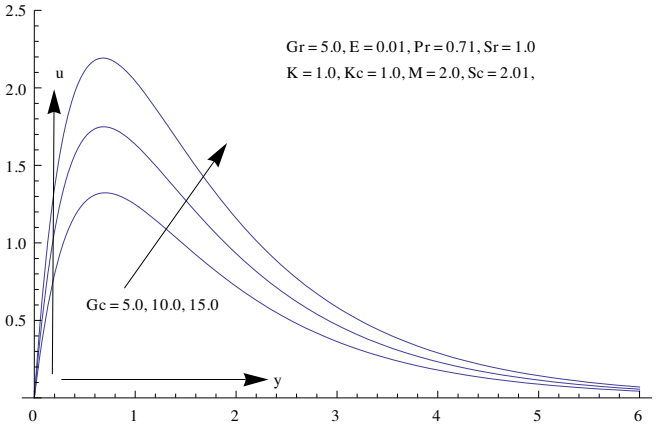

Figure-4: Velocity profiles for different Gc

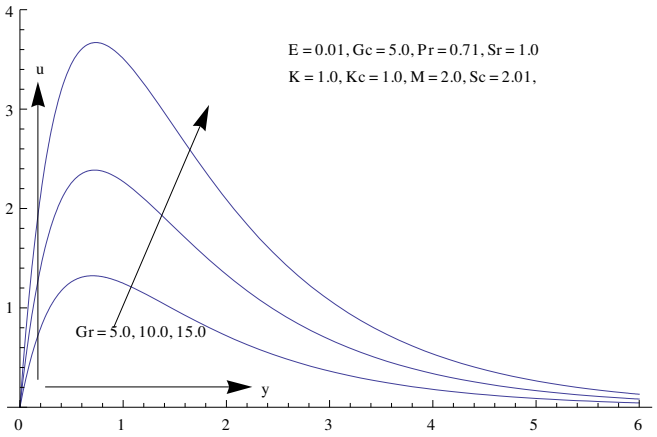

Figure-5: Velocity profiles for different Gr

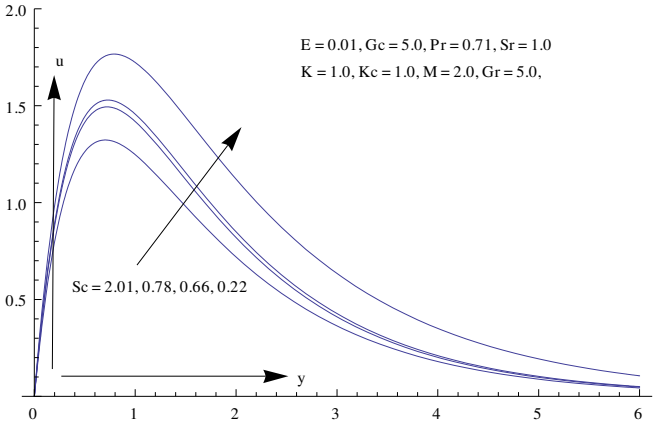

Figure-6: Velocity profiles for different Sc

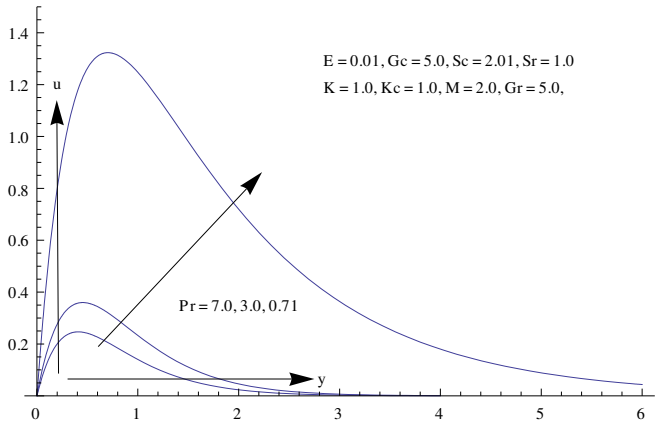

Figure-7: Velocity profiles for different Pr

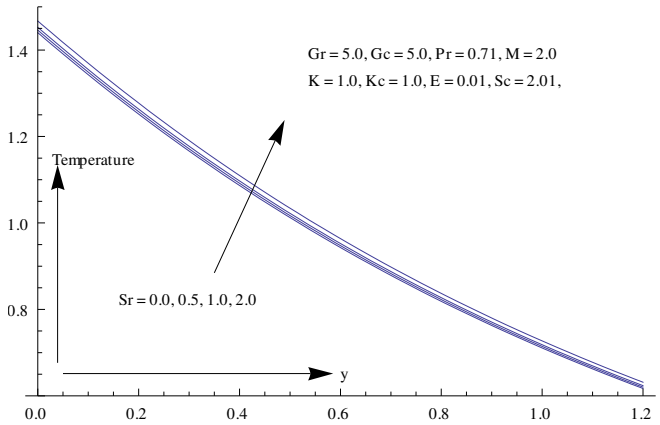

Figure-10: Temperature profiles for different Sr

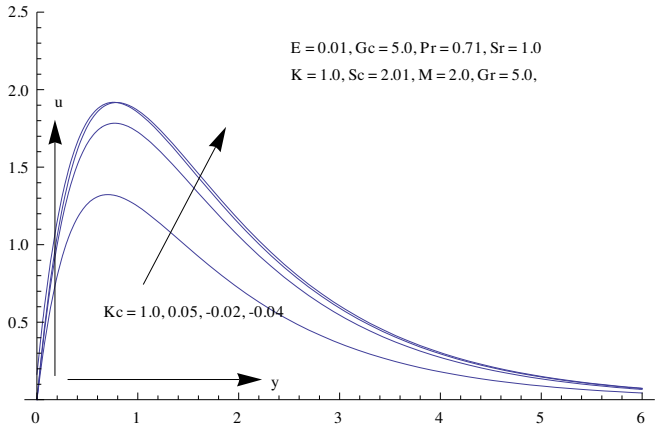

Figure-8: Velocity profiles for different Kc

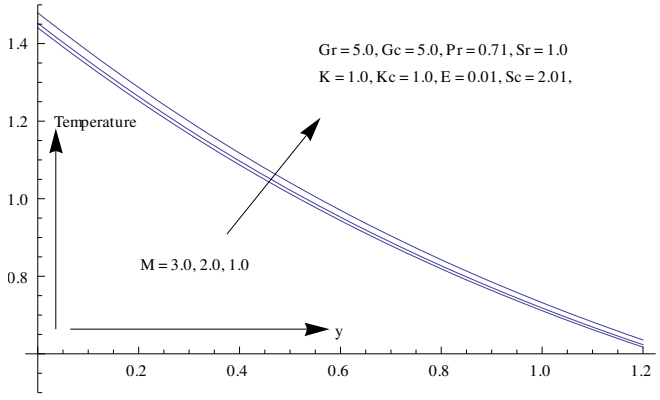

Figure-11: Temperature profiles for different M

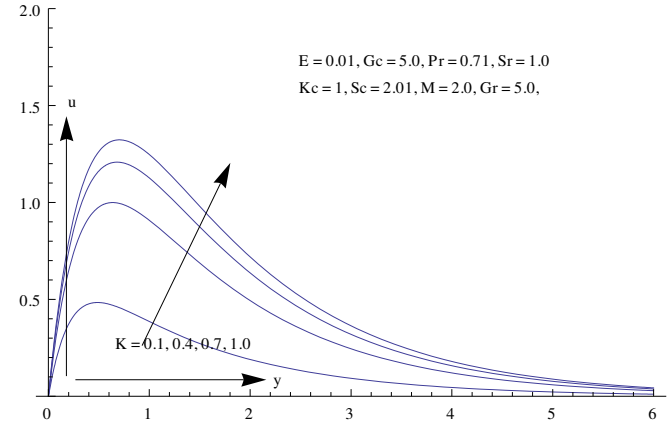

Figure-9: Velocity profiles for different K

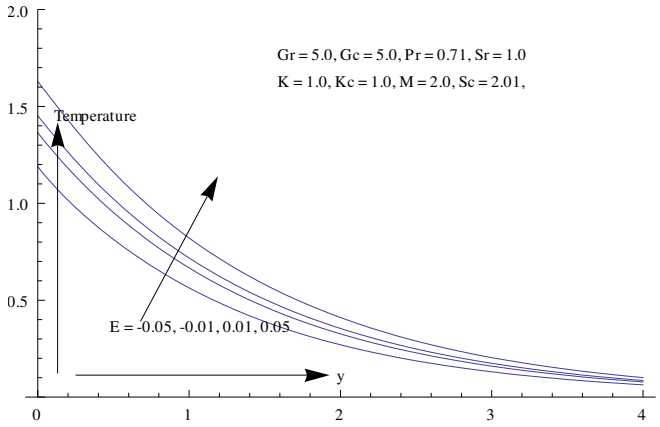

Figure-12: Temperature profiles for different E

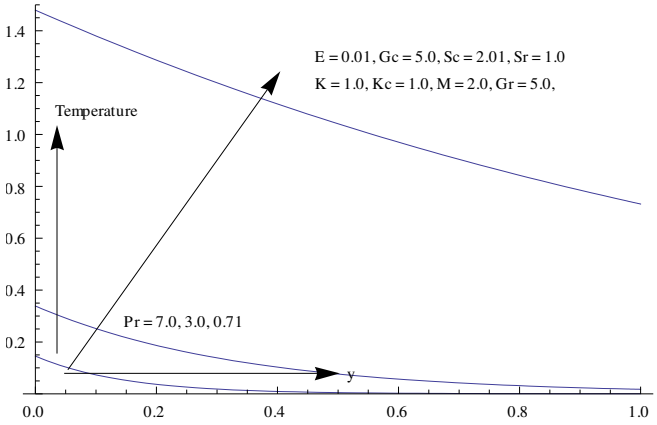

Figure-13: Temperature profiles for different Pr

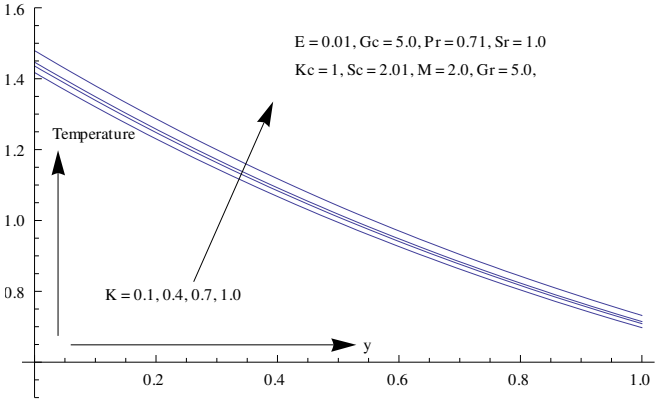

Figure-14: Temperature profiles for different K

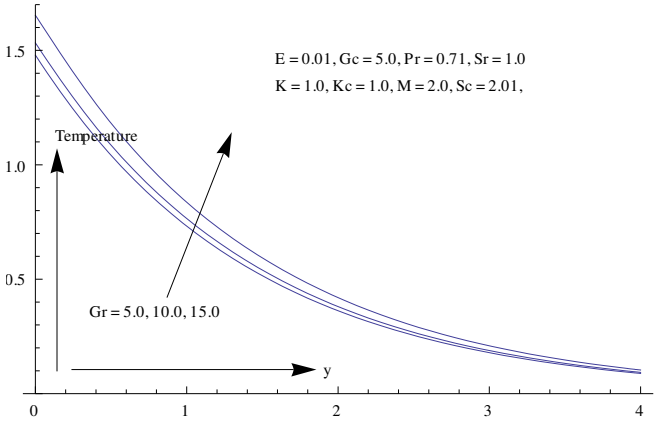

Figure-15: Temperature profiles for different Gr

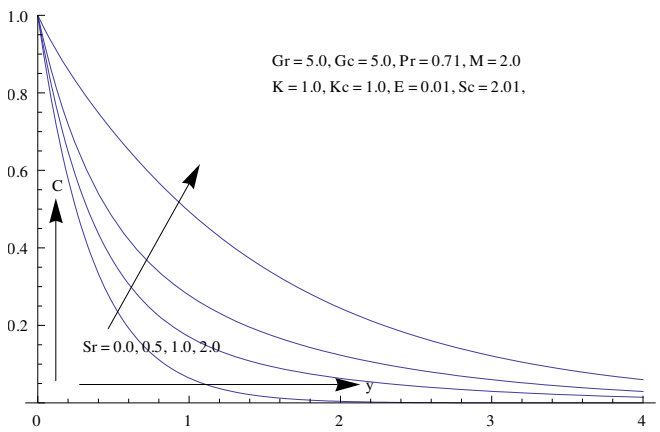

Figure-16: Concentration profiles for different Sr

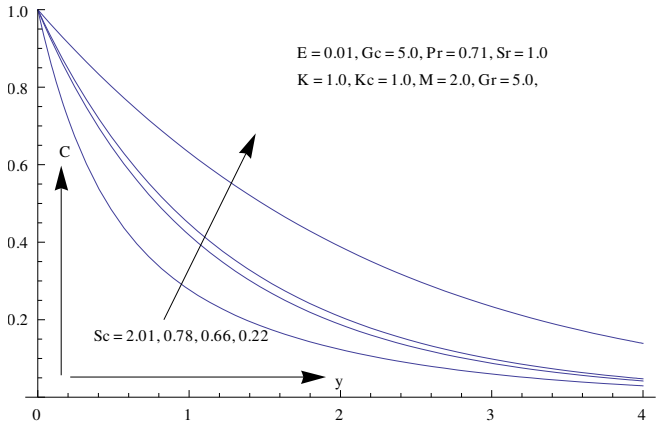

Figure-17: Concentration profiles for different Sc

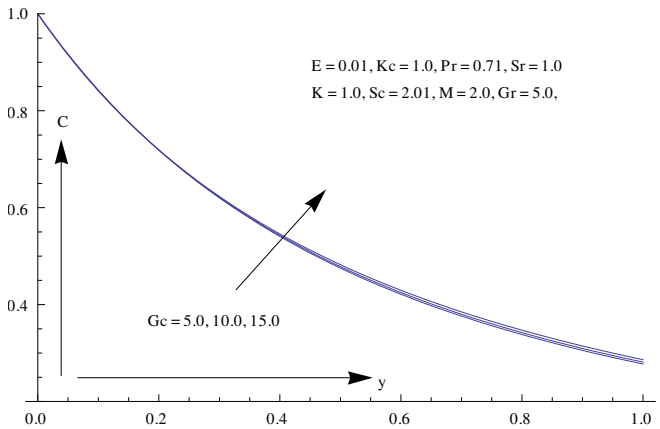

Figure-18: Concentration profiles for different Gc

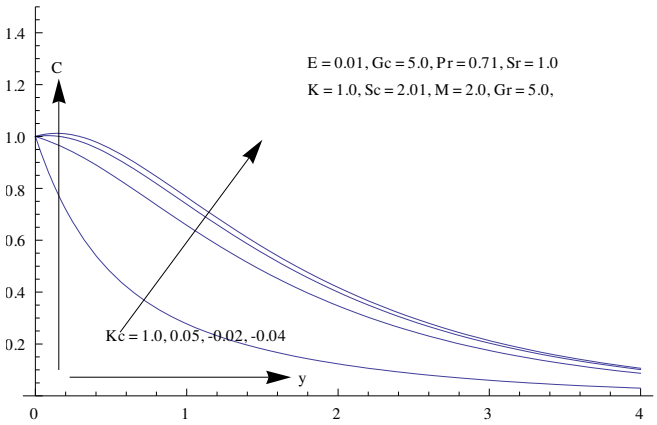

Figure-19: Concentration profiles for different Kc

Table-1: Skin-friction for different Sr

M	Sr	Kc	E	Pr	Sc	K	Gr	Gc	τ	Sh
2.0	0.0	1.0	0.01	0.71	2.01	1.0	5.0	5.0	4.82183	2.74282
2.0	0.5	1.0	0.01	0.71	2.01	1.0	5.0	5.0	5.14653	2.25989
2.0	1.0	1.0	0.01	0.71	2.01	1.0	5.0	5.0	5.47418	1.78080
2.0	2.0	1.0	0.01	0.71	2.01	1.0	5.0	5.0	6.13248	0.836088

Table-2: Skin-friction for different E

M	Sr	Kc	E	Pr	Sc	K	Gr	Gc	τ
2.0	1.0	1.0	0.05	0.71	2.01	1.0	5.0	5.0	6.00278
2.0	1.0	1.0	0.01	0.71	2.01	1.0	5.0	5.0	5.47418
2.0	1.0	1.0	-0.01	0.71	2.01	1.0	5.0	5.0	5.20988
2.0	1.0	1.0	-0.05	0.71	2.01	1.0	5.0	5.0	4.68128

Table-3: Skin-friction for different K

M	Sr	Kc	E	Pr	Sc	K	Gr	Gc	τ
2.0	1.0	1.0	0.01	0.71	2.01	1.0	5.0	5.0	5.47148
2.0	1.0	1.0	0.01	0.71	2.01	0.7	5.0	5.0	5.17617
2.0	1.0	1.0	0.01	0.71	2.01	0.4	5.0	5.0	4.61588
2.0	1.0	1.0	0.01	0.71	2.01	0.1	5.0	5.0	3.01474

Table-4: Skin-friction for different Sc

M	Sr	Kc	E	Pr	Sc	K	Gr	Gc	τ	Sh
2.0	1.0	1.0	0.01	0.71	2.01	1.0	5.0	5.0	5.47148	1.78080
2.0	1.0	1.0	0.01	0.71	0.78	1.0	5.0	5.0	5.94204	0.936298
2.0	1.0	1.0	0.01	0.71	0.66	1.0	5.0	5.0	6.02521	0.844031
2.0	1.0	1.0	0.01	0.71	0.22	1.0	5.0	5.0	6.52579	0.45714

Table-5: Skin-friction for different Pr

M	Sr	Kc	E	Pr	Sc	K	Gr	Gc	τ
2.0	1.0	1.0	0.01	0.71	2.01	1.0	5.0	5.0	5.47148
2.0	1.0	1.0	0.01	3.0	2.01	1.0	5.0	5.0	2.08670
2.0	1.0	1.0	0.01	7.0	2.01	1.0	5.0	5.0	1.59966

Table-6: Skin-friction for different M

M	Sr	Kc	E	Pr	Sc	K	Gr	Gc	τ
3.0	1.0	1.0	0.01	0.71	2.01	1.0	5.0	5.0	4.22286
2.0	1.0	1.0	0.01	0.71	2.01	1.0	5.0	5.0	5.47418
1.0	1.0	1.0	0.01	0.71	2.01	1.0	5.0	5.0	6.46882

Table-7: Skin-friction for different Kc

M	Sr	Kc	E	Pr	Sc	K	Gr	Gc	τ	Sh
2.0	1.0	1.0	0.01	0.71	2.01	1.0	5.0	5.0	5.47148	1.78080
2.0	1.0	0.05	0.01	0.71	2.01	1.0	5.0	5.0	6.62476	0.184482
2.0	1.0	-0.02	0.01	0.71	2.01	1.0	5.0	5.0	6.72725	-0.082293
2.0	1.0	-0.04	0.01	0.71	2.01	1.0	5.0	5.0	6.93766	-0.168965

Table-8: Skin-friction for different Gr

M	Sr	Kc	E	Pr	Sc	K	Gr	Gc	τ
2.0	1.0	1.0	0.01	0.71	2.01	1.0	5.0	5.0	5.47418
2.0	1.0	1.0	0.01	0.71	2.01	1.0	10.0	5.0	9.55888
2.0	1.0	1.0	0.01	0.71	2.01	1.0	15.0	5.0	14.4391

Table-9: Skin-friction for different Gc

M	Sr	Kc	E	Pr	Sc	K	Gr	Gc	τ
2.0	1.0	1.0	0.01	0.71	2.01	1.0	5.0	5.0	5.47418
2.0	1.0	1.0	0.01	0.71	2.01	1.0	5.0	10.0	7.42462
2.0	1.0	1.0	0.01	0.71	2.01	1.0	5.0	15.0	9.44930